Imperfection Induced Wrinkling Material Failure in Sandwich Panels

Linus Fagerberg and Dan Zenkert
KTH Aeronautical and Vehicle Engineering
SE-100 44, Stockholm, Sweden
E-mail: linus@kth.se, danz@kth.se

Abstract: In this paper sandwich wrinkling, or local face sheet instability, is treated in the context of material failure. Traditionally, test results rarely comply well with the predicted failure load and a knockdown factor often has to be used. The reason for this is often referred to being the effect of initial geometrical imperfections. In this paper, imperfections are included in the form of the natural waveform given by the linear stability analysis, i.e., a short wavelength sinusoidal buckling shape. These initial imperfections lead to increased displacements during loading giving rise to both in-plane compressive strain and a varying bending strain. These strains can then be related to material failure criteria, one for the face sheet compressive strain and one for the core normal strain. An analytical model is derived and compared to experimental results and several issues are revealed. Using a realistic initial imperfection amplitude, the measured panel strength agrees very well with the derived model, giving a prediction somewhat below the values obtained from the traditional approach. This verifies that the actual wrinkling failure is below the theoretical instability load. Secondly, the model is able to distinguish between different failure modes, face sheet compression failure or core/adhesive joint tensile failure, giving good correlation with experimental findings. Thus, it appears that using initial imperfections as a basis for wrinkling analysis provides a better foundation for failure analysis than ordinary stability analysis, and it also allows to determine what failure mode is predominant. Finally, it is shown that the choice of core material can be done based on the theory presented to obtain a more efficient sandwich panel.

Keywords: wrinkling, local buckling, imperfection, stability, sandwich

Introduction

In the design of sandwich structures, low weight is often the primary objective. For this reason, a design with minimum weight is sought satisfying all the design constraints. For sandwich structures the number of design constraints is commonly quite large due to the combination of different materials. Therefore, global constraints such as stiffness, natural frequency or overall stability have to be considered along with local material strength based

criteria. For a sandwich such criteria can be; face sheet tension or compression failure, core shear failure, face/core adhesive joint failure, local indentation, impact, wear, etc. The mechanical constraints could both be considered for static, dynamic or fatigue loading. Along with these constraints wrinkling, or local face sheet instability, is often included as a strength requirement. The reason for this is that this form of instability, as treated in e.g. [1-2], results in an expression for the wrinkling load or stress that is only a function of the face sheet local bending stiffness and the stiffness properties of the core (the elastic foundation). This implies that the wrinkling load or stress can be applied in the design process as a constraint for the face sheet compressive load bearing capacity, being active if the wrinkling stress is lower than the face sheet compressive failure strength. Synthesised models for global and local (wrinkling) instability, including the transition between global and local buckling modes also exist, e.g. [3]. However, it is not the objective of this study to pursue along these lines of investigation, but to move from a stability criteria to a more physically correct materials strength criteria.

Background and problem statement

Going back to the early work on wrinkling summarised in [1,2,4] we can make the following short flashback. The wrinkling problem was defined as a beam or strut (the face sheet) resting on an elastic foundation, as depicted in Figure 1. In these and subsequent studies on the subject, e.g., [5], the assumptions are that the face sheet and the core are linear elastic and isotropic materials, and that it assumes a thin strut or plate in cylindrical bending subjected to a uniaxial compressive load. Extensions of this type of analysis towards more general plate problems with generally anisotropic face sheets, orthotropic cores and multi-axial loading have been studied in [6-8], still based on linear elastic material behaviour and focusing on the stability problem.

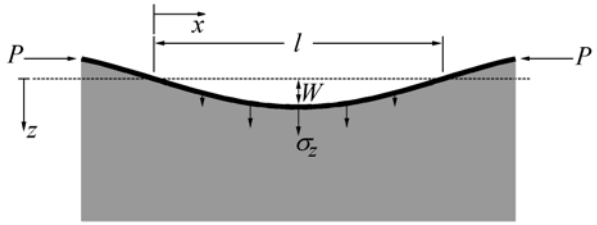

Figure 1. The basic wrinkling wave.

For a beam or a plate in cylindrical bending (the face sheet), the governing differential equation reads

$$D_f \frac{d^4 w}{dx^4} + P \frac{d^2 w}{dx^2} - \sigma_z = 0 \tag{1}$$

where D_f is the bending stiffness of the face sheet alone, P is the compressive load (per unit width) acting on the face sheet and σ_z the support pressure from the core, the elastic foundation. There are several different cases of wrinkling. These are depicted in Figure 2.

Figure 2. Wrinkling modes; Case I, Case II and Case III.

All three wrinkling modes have previously been examined by several authors, e.g. [1,2,4]. A unified theoretical approach to describe and solve these three modes has also been presented by Niu and Talreja [5]. The first mode, which is called "Case I" or "Rigid base", may occur in bending when only one of the face sheets is subjected to compression or in pure compression when the sandwich has unsymmetric face sheets with different wrinkling loads.

The second mode, "Case II" or "Snake" mode, is not a true local phenomenon and should not be solved using wrinkling formulae. The middle plane of the core does not remain undeformed and the thickness of the core is of significant importance both to the natural wavelength and to the critical load. This type of instability is better captured by formulae for global buckling, where the overall dimensions of the sandwich are included. It is only active for very narrow plate problems. As soon as the problem is of beam type (without supported unloaded edges) this type of thin sandwich suffers from global buckling. Even a sandwich with honeycomb or other anisotropic core material with a high out-of-plane Young's modulus to shear modulus ratio, that is prone to fail in Case II wrinkling, is much more likely to have an even lower global stability failure load.

The third mode, "Case III" or "hourglass" mode, is basically a special case of Case I wrinkling that will never appear in reality. If the sandwich is thin so that stability of one face sheet is affected by the other, the Case III mode gives a shorter natural wavelength and a higher stability failure load than both other cases.

If the core is sufficiently thick all three modes predict the same failure load, simply because one face sheet remains unaffected by the other and characteristics such as critical wavelength and wrinkling load are governed by material properties alone. This fundamental or "basic wrinkling" case is the most "to the point" description of the local stability failure problem we wish to investigate. The key to successfully design a sandwich beam or plate is to first design against this basic case of wrinkling failure (thick core) and thereafter also make sure that global buckling is accounted for. The formulae for Case I, Case II and Case III wrinkling are only interesting from a theoretical point of view. Hence all the following sections of this paper will only consider the basic wrinkling case.

One of the most straight-forward approaches to describe sandwich wrinkling is to model the core as a Winkler foundation. Formulae derived on that assumption are commonly known, but have shown to give poor predictions for foam core sandwich beams and panels and will not be covered in this paper.

Among the first to comprehensively study the wrinkling problem were Hoff and Mautner [1] and their analysis resulted in a design formula that could be used to predict the critical face stress associated with the wrinkling phenomena. These equations and all others presented in this paper are expressed per unit width and per face sheet if not specified otherwise.

$$P_{Hoff} = 0.91 t_f \sqrt[3]{E_f E_c G_c} \text{ or } \sigma_{Hoff} = 0.91 \sqrt[3]{E_f E_c G_c} \tag{2}$$

where E_f is the isotropic face sheet modulus, t_f the face sheet thickness and E_c and G_c are the core normal and shear moduli, respectively. These relations were derived for the case of thick cores (basic wrinkling). The factor 0.91 in these relations were later knocked down to 0.5 in order to correlate with experiments. This formula is still used in the industry today (using the factor 0.5 in front of the third root expression). This was suitable in the early days when sandwich panels used to have isotropic face sheets manufactured from metal or quasi-isotropic fibre reinforced face sheets. It does not include the effect of through-the-thickness anisotropy of, for example, face sheets manufactured from a few layers of uni-directional fabrics. Later, Plantema [2] published an improved theory; the difference being that instead of assuming an isotropic, homogeneous face sheet material, the face sheet was described by its local bending stiffness and instead of a linear through-the-thickness stress decay an exponential decay function was used, similar to most shear lag problems. The resulting formula, however, has a similar form described by

$$P_{Plantema} = \frac{3}{2} \sqrt[3]{2 D_f E_c G_c} \tag{3}$$

where, if the face sheet is isotropic

$$D_f = \frac{E_f t_f^3}{12} \text{ for a narrow beam or} \tag{4}$$

$$D_f = \frac{E_f t_f^3}{12(1-\nu_f^2)} \text{ for a plate in cylindrical bending} \tag{5}$$

If the face sheet is not isotropic D_f is calculated using laminate theory, see e.g. Zenkert [9]. Inserting Equation (4) and (5) into Equation (3) gives

$$\sigma_{Plantema} = 0.825 \sqrt[3]{E_f E_c G_c} \text{ for a narrow beam or} \tag{6}$$

$$\sigma_{Plantema} = 0.85 \sqrt[3]{E_f E_c G_c} \text{ for the plate (with } \nu_f = 0.3\text{).} \tag{7}$$

It is obvious that the formula by Plantema is very similar to the one presented by Hoff and Mautner. The different assumptions only change the constant term in the front of the cubic root expression. Plantema's formula, Equation (3) includes the effect of the bending stiffness and is more suited for the anisotropic face sheets of today's sandwich structures.

A few years after Plantema, Allen [4] solved the wrinkling problem by solving the governing differential equation and assuming that the core stress field has to satisfy the Airy's stress function under 2D conditions (beam or plate in cylindrical bending). From this he derived the core stress at the interface between the core and face sheet $(z = 0)$, as

$$\sigma_z = -\frac{a}{l} w_m \sin\left(\frac{\pi x}{l}\right) \text{ with } a = \frac{2\pi E_c}{(3-\nu_c)(1+\nu_c)} \tag{8}$$

This leads to the following expressions for the natural wavelength and wrinkling load

$$l = \sqrt[3]{\frac{2\pi^4 D_f}{a}} \text{ and } P_{Allen} = \left(\frac{1}{2^{\frac{2}{3}}} + 2^{\frac{1}{3}} \right) \frac{1}{\pi^2} \sqrt[3]{D_f a^2} \approx 0.88 \sqrt[3]{D_f a^2} \tag{9}$$

If the face sheet is isotropic the bending stiffness can be substituted as shown above, the resulting formulae for the wrinkling wavelength and critical stress are obtained as

$$l = \pi t_f \sqrt[3]{\frac{(3-\nu_c)(1+\nu_c)E_f}{12(1-\nu_f^2)E_c}} \text{ and } \sigma_{Allen} = \frac{3}{\sqrt[3]{12(3-\nu_c)^2(1+\nu_c)^2}} \sqrt[3]{E_f E_c^2} \tag{10}$$

For a core material with Poisson's ratio ν_c=0.3 the approaches by Hoff and Mautner, Plantema and Allen compare as

$$\sigma_{Hoff} = 0.91 \sqrt[3]{E_f E_c G_c} = \left\{ G_c = \frac{E_c}{2.6} \right\} = 0.66 \sqrt[3]{E_f E_c^2} \tag{11}$$

$$\sigma_{Plantema} = 0.825 \sqrt[3]{E_f E_c G_c} = \left\{ G_c = \frac{E_c}{2.6} \right\} = 0.60 \sqrt[3]{E_f E_c^2} \tag{12}$$

$$\sigma_{Allen} = \frac{3}{\sqrt[3]{12(3-\nu_c)^2(1+\nu_c)^2}} \sqrt[3]{E_f E_c^2} = 0.58 \sqrt[3]{E_f E_c^2} \tag{13}$$

from which it is rather obvious that all three approaches give very similar results. In the perspective of the analyst or designer, any of these could be used. However, as pointed out by Hoff and Mautner [1] the derived analytical expression may provide the correct predictions in terms of trends but are commonly non-conservative and an appropriate knock-down factor should be used. There are many reason for the analytical expressions to be non-conservative. The most obvious one is general for all stability problems solved with linear methods – there is no account for any type of initial imperfections. Most reported experimental results on wrinkling failure of sandwich panels, show that the classical wrinkling formulae provides the correct trends but with a non-conservative load or stress prediction, e.g. [1,10,11.]

The results given by Allen [4] are believed more reliable than those presented by Hoff and Mautner [1] and Plantema [2], since the assumptions regarding the core stress fulfil the equilibrium equations. Allen's results will therefore be used in the rest of this paper.

In stability analysis one often considers different cases. The classical case is linear buckling analysis, or bifurcation analysis. In cases where the structure has no, or at least very small imperfections, the deformations prior to buckling are often considered negligible. In such cases, linear buckling analysis suffices. Such a case is shown in Figure 3 (straight line). Classical wrinkling analysis and design formulae are based on such assumptions. In cases of non-negligible imperfections, the pre-buckling deformations will be significant leading to a kinematically non-linear problem. In the case of a strut, this means that the out-of-plane deformation will increase non-linearly with the applied in-plane load. Buckling can in some cases be defined by the point where the out-of-plane deformations starts to increase rapidly with an increment in the applied in-plane load or when an increased out-of-plane deformation leads to a decrease in load, denoted "limit load" (Figure 3, curved line). Any analysis of such

points are based on the estimation of load, or deformation, states that lead to some or even all terms in the stiffness matrix being zero.

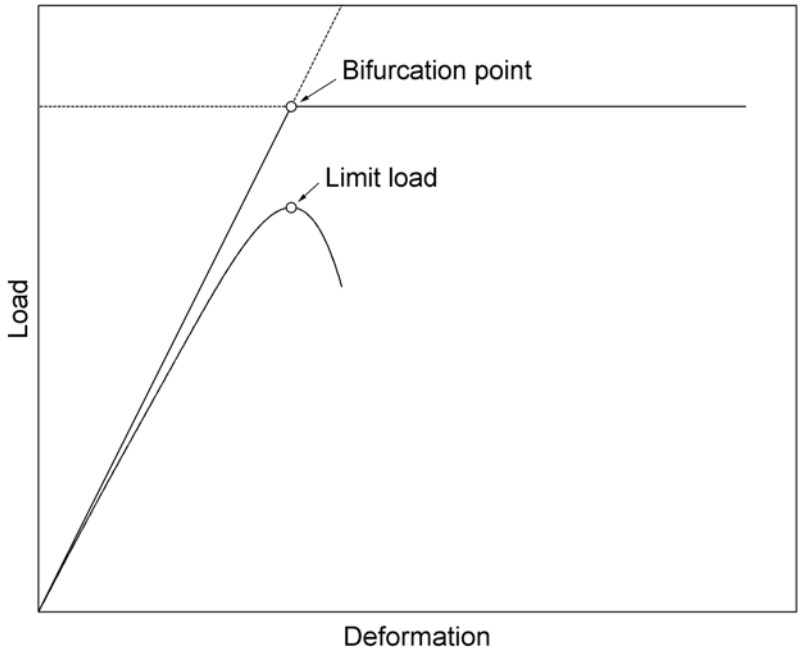

Figure 3. Bifurcation and limit load

Whichever of these cases occurs, there is one further issue to consider, and that is material failure. What if, somewhere along the load-deformation (equilibrium) path in the non-linear case, stresses lead to a material failure? In the wrinkling case the sandwich panel may then suffer from face sheet compression failure prior to instability. In this context the aim of the present paper is to study material failure appearing in a compression loaded sandwich panel having some initial imperfections.

Theoretical Approach

Sandwich panels are often described as imperfection sensitive. We may approach this by assuming a small local imperfection of some shape and amplitude. However, it is more convenient to assume that the imperfection has the same shape as the natural wrinkling pattern with an initial amplitude W_0 and length l. This is perhaps not strict in a practical sense, but it would be a conservative estimate. Furthermore, this is the shape the panel "wishes" to assume leading to a minimum energy state. The initial shape of the sandwich face sheet is therefore described as

$$w_0 = W_0 \sin\left(\frac{\pi x}{l}\right) \tag{14}$$

If we apply an in-plane compressive load to a strut or plate with an initial imperfection of this kind, we can use a linear approach to find the new total deformation w_t as

$$w_t = \frac{w_0}{1-\frac{P}{P_{cr}}} \tag{15}$$

which is also valid for a strut or plate on an elastic foundation [4]. This equation has also been derived by Timoshenko [12] and Brush and Almroth [13]. The difference (or increase) in the wrinkling wave w_m is the difference between the total wrinkling wave after loading w_t and the initial wave w_0

$$w_m = w_t - w_0 \tag{16}$$

The change in wavelength is thereby neglected, implying that the derived formulae for the failure load will give a somewhat non-conservative result.

By using the relations described in Equations (14-16) the change of wrinkling waveform can be expressed as

$$w_m = \frac{w_0}{1-\frac{P}{P_{cr}}} - w_0 = \frac{P}{P_{cr}-P} w_0 = W_0 \frac{P}{P_{cr}-P} \sin\left(\frac{\pi x}{l}\right) \tag{17}$$

Thus the equilibrium path for the imperfect sandwich is known and can be plotted in the P/P_{cr}-W_m space for different imperfection amplitudes (see examples depicted in Figure (4)). Here W_m is the effective wrinkling amplitude, being the difference between the total wrinkling amplitude W_t and the initial imperfection amplitude W_0 (compare with Equation (16)).

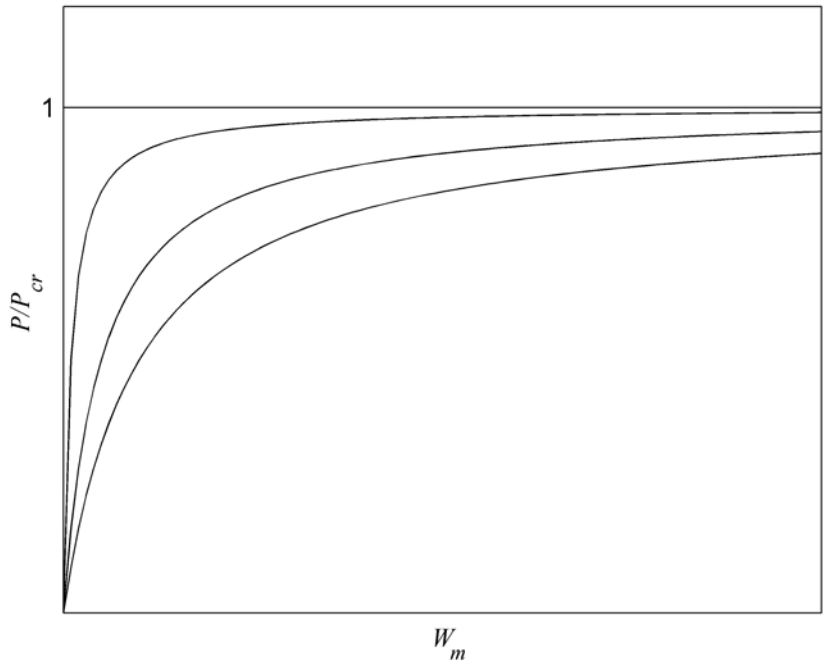

Figure 4. Equilibrium paths in the P/P_{cr} -W_m. space for different imperfection amplitudes.

The next step is to consider points on this load-deformation path where the different constituent materials may fail. As previously pointed out, the local loss of stability is often considered as a failure criteria which is dependent on the material combination and the design

variables. Usually wrinkling and face compression failure are investigated as two different failure modes and the lowest of the two is taken as the estimated failure load to be used as a design constraint for face sheet compression. The compressively loaded imperfect sandwich can fail in two distinct ways; face sheet failure or core/adhesive joint failure. In the case of a perfectly straight panel, the face sheet compression stress is simply when the far field compressive stress reaches the laminate compressive strength, since one assume no local face sheet bending. In the case of an initially imperfect panel, the deformation causes an additional curvature of the face sheet, giving a locally varying bending moment and bending stresses over the thickness of the face sheet. These would vary from tensile to compressive along the face sheet and over the thickness. One would not expect a core failure in a perfectly straight panel, but for one with initial imperfections, local tensile and compressive stresses, normal to the face sheet, will build up as a result of the increasing out-of-plane deformation and may cause core failure. The most critical areas in a compressed imperfect sandwich are where the core and face stresses are highest. It is quite easy to understand that the maximum stress in the core occurs at the face-core interface, at the location where the wrinkling wave reaches its peak or bottom, see (A) and (B) in Figure 5. The compressive stress in the face sheet is highest at the inside of the face sheet in point (A) or outside in point (B), Figure 5.

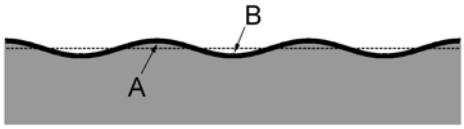

Figure 5. Critical areas in the compression loaded imperfect sandwich.

The preferred case is often to have face failure occur as the critical failure mode, at a load level close to the pure compression failure load of the face sheet. Thus the expensive face sheet is used to its fullest and gives the most “value for the money spent”. The second failure mode where the core is the critical constituent is undesirable and can occur at a load levels much lower than the face sheet compression failure load if the combination of core and face material is not thought through properly. In theory it is possible to get core compression failure but in practice it is much more common to get core tension failure, which is quite abrupt and the face sheet virtually ruptures away from the core.

Face compression failure

The face sheet material is assumed to be able to sustain a certain compression strain $\hat{\varepsilon}_f$. Hooke’s law then gives the relation (P is the applied compressive load per unit width)

$$\varepsilon_f^c = \frac{P}{t_f E_f} \tag{18}$$

and maximum load is calculated from

$$\hat{P} = t_f E_f \hat{\varepsilon}_f^c \tag{19}$$

where $\hat{\varepsilon}_f^c$ is the strain at which the face sheet fails in compression.

Imperfection introduced face bending failure

The strain in the face sheet that arises from bending (wrinkling) varies both through the thickness of the face sheet and along the length of the face sheet. It can be described according to ordinary beam bending theory as

$$\varepsilon_f^b = -\frac{M}{D_f} z = z\frac{d\,w^2}{d\,x^2} = z(w_t - w_0)\frac{\pi^2}{l^2}\sin(\frac{\pi\,x}{l}) \tag{20}$$

The maximum local face strain in the bent configuration is obviously at the boundary of the face sheet ($z = \pm t_f / 2$), and where the curvature of the face sheet has a maximum ($x = \pm l / 2$), see Figure 1 and 5. Hence the maximum local strain in the face sheet is

$$\hat{\varepsilon}_f^b = \frac{\pi^2 t_f}{2l^2}(w_t - w_0) \tag{21}$$

If the face sheet is not isotropic and, e.g. one of the outer plies consists of a high strain material, a different local coordinate z must be used. If for example a [90/0]s face sheet is studied $z = \pm t_f/4$ should be used in order to predict compressive failure in the 0-degree layer. This is in fact the "first ply failure" criterion that can be implemented fully in the described theory. In order to not complicate the following text and examples more then necessary, the first ply failure technique is not further mentioned but the reader should be aware of its existence.

By using Equation (17) Equation (21) can be rewritten as

$$\varepsilon_f^b = \frac{\pi^2 t_f}{2l^2} w_0 \frac{P}{(P_{cr} - P)} \tag{22}$$

Hence the total maximum face strain is the sum of the strain from the bent and straight configurations (Equation(18) and Equation(22) respectively).

$$\varepsilon_f = \frac{\pi^2 t_f}{2l^2} w_0 \frac{P}{(P_{cr} - P)} + \frac{P}{t_f E_f} \tag{23}$$

Imperfection introduced core wrinkling failure

The face-core interface normal stress is, according to Allen [4], given in Equation (8). The maximum interface normal stress is therefore equal to

$$\sigma_{z\max} = -\frac{a}{l} w_m = \frac{a}{l}(w_t - w_0) \text{ with } a = \frac{2\pi E_c}{(3 - v_c)(1 + v_c)} \tag{24}$$

so that the maximum strain in the core is

$$\varepsilon_c = \frac{\sigma_z}{E_c} = \frac{a}{l\,E_c}(w_t - w_0) = \frac{a}{l\,E_c} W_0 \frac{P}{P_{cr} - P} \tag{25}$$

Which gives the critical load with respect to core failure

$$\hat{P}_c = \frac{P_{cr}}{1 + \frac{a W_0}{l E_c \hat{\varepsilon}_c}} \tag{26}$$

And the critical effective imperfection amplitude

$$\hat{W}_m = \frac{l E_c \hat{\varepsilon}_c}{a} \tag{27}$$

The critical effective wrinkling amplitude is constant and unaffected by the initial imperfection amplitude and a function of the material properties and thicknesses alone.

Failure prediction procedure

Using Equation (26) and Equation (27) core failure can be directly evaluated while for the face sheet a different, iterative approach has to be used. Using Equation (17) we increase the applied in-plane load P to calculate the added deformation W_m for a given initial imperfection amplitude W_0. At each load step, we check the face strain according to Equation (23) being superimposed by a far field compressive stress from the applied in-plane load and a local maximum bending stress resulting from the initial imperfection w_0. Failure will then occur at the lower of the two loads predicted for the core and face respectively. This method obviously also provides means to determine which type of failure is most likely to occur.

Example calculations

We shall now make a number of trial calculations using the derived model. The first example considers a sandwich beam with 1 mm thick uni-directional carbon reinforced composite face sheets on a core with a Young's modulus similar to that of the Divinycell H60 core material, 56 MPa and a Poisson's ratio of 0.3. The face sheet has an in-plane modulus of 107 GPa in the load direction and is assumed to have a compressive failure strain $\hat{\varepsilon}_f$ equal to 0.008 (0.8%). Two different critical strains are used for the core; both a high failure strain of 0.1 (10%) similar to PVC material from the Divinycell H-grade series (ductile core), and the other used failure strain was 0.033 (3.3%), which is similar to typical failure strains of PMI foam core material found for the Rohacell WF-grade material series (brittle core).

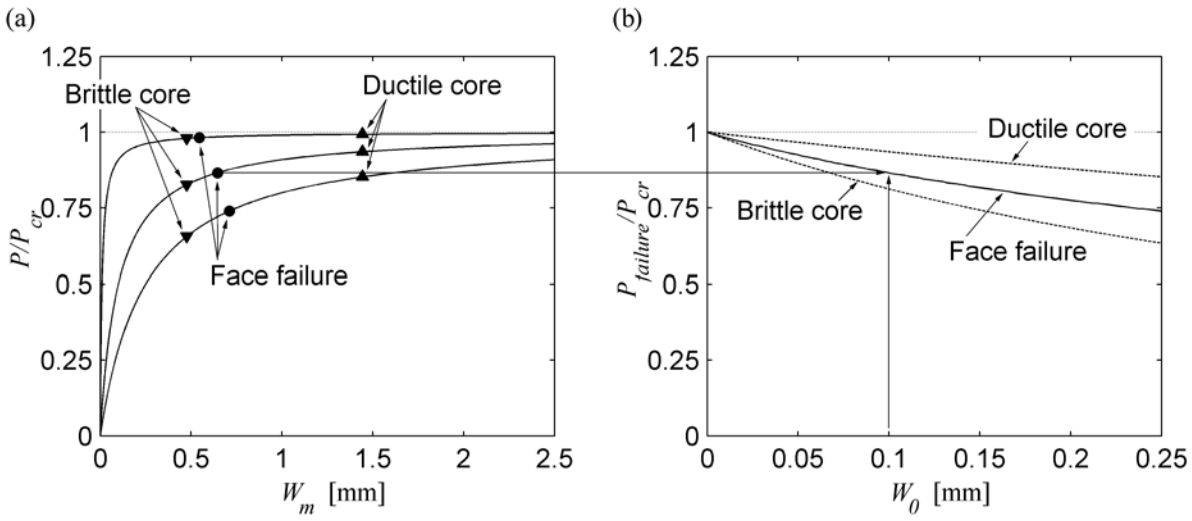

Figure 6. Example for a sandwich beam with1 mm UD Carbon and H60.
(a) Equilibrium paths for various imperfection amplitudes of 0.01, 0.1 and 0.25 mm.
(b) Face and core failure envelopes vs. initial imperfection amplitudes.

In Figure 6a, the equilibrium paths for different initial imperfection amplitudes are shown, 0.01, 0.1 and 0.25 mm. The value of the in-plane load P is normalised with respect to the wrinkling load of the face sheet, Equation (9), for a perfectly straight column. As seen in these equilibrium paths, increasing the initial imperfection reduces the stiffness of the beam. In Figure 6a, circular dots are included representing values for face failure. Core failure is indicated with the filled triangles. The high failure strain is represented with the triangles pointing upwards and the lower failure strain by triangles pointing downwards. In the figure it can be seen that if the core is relatively brittle (PMI) it is expected to fail by core rupture and if it is ductile (PVC) it will probably fail by face fracture. It is clearly seen that the value of the in-plane load at failure depends on the amplitude of the assumed initial imperfection. For small imperfections, the load is very close to the wrinkling load (top solid line in Figure 6a), but with increasing initial amplitude, the load is reduced. It can further be seen that a line drawn through each group of core failure is vertical. Or in other words, core failure occurs at a constant effective wrinkling amplitude. This can also be seen directly in Equation (27). A virtual line through the markers for face failure is not vertical but rather inclined and not purely straight. Extending this line upward would make it cross the load axis at the compression failure load of the face sheet for W_0 equal to zero. In Figure 6b, the normalized predicted failure load for face sheet compression failure and core failure (both brittle and ductile) are sketched as function of the initial imperfection amplitude. The arrow crossing from Figure 6a to 6b shows how the lines in Figure 6b are constructed. As seen, in this example, core failure always occurs before face failure if a brittle core is used, regardless of imperfection amplitude. If on the other hand a ductile core is used the failure mode would be face failure. For reasonable imperfection amplitudes, say 0.1 mm, the failure load is approximately 85% of the wrinkling load if a ductile core is used. This means that for this particular configuration the analytical expression in Equation (9) should be knocked down and multiplied by approximately 0.85. However, this knock-down depends both on the imperfection amplitude, the configuration and the materials used. For large initial imperfection amplitudes, and this material combination, the failure load goes down to 70% or less of the wrinkling load.

Increasing the core modulus to 105 MPa (same as Divinycell H100) and using the same face sheet and critical strains as in the previous example gives the results displayed in Figure 7a and 7b.

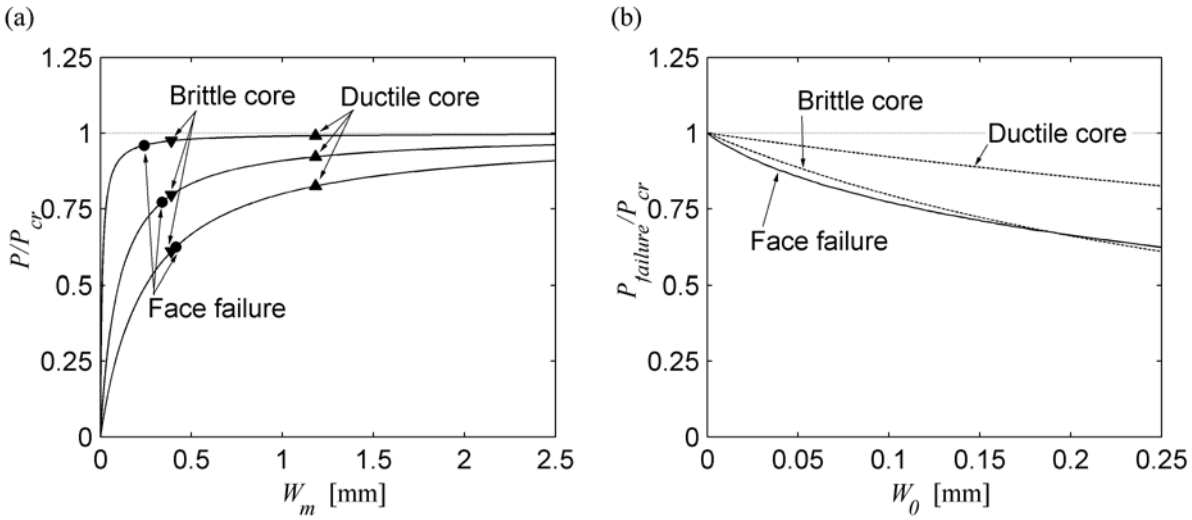

Figure 7. Example for a sandwich beam with 1 mm UD Carbon and H100.
(a) Equilibrium paths for various imperfection amplitudes of 0.01, 0.1 and 0.25 mm.
(b) Face and core failure envelopes vs. initial imperfection amplitudes.

For this material combination face sheet failure occurs before ductile core failure for all reasonable initial imperfection amplitudes but brittle core failure precedes face failure only for large imperfections and not for small. The shift in failure mode occurs for an initial imperfection amplitude of approximately 0.2 mm. By comparing Figure 6a and 7a it can be seen that increasing the core modulus shifts the predicted failure markers to the left, towards smaller effective wrinkling amplitudes. Another interesting observation is that even for moderate imperfections (0.25 mm is about 25% of the face sheet thickness), the failure load is only about 60-65% of the theoretical wrinkling load. This means that the factor preceding the cubic root sign in Equation (9) should be knocked down considerably. Actually, these results indicate that the knock down is in the order of what Hoff and Mautner [1] suggested, based on their early experimental work.

By further increasing the core modulus to 230 MPa (Divinycell H200) the pure compressive failure load of the face sheet is lower then the wrinkling load and this changes the appearance of the graphs, see Figure 8a and 8b.

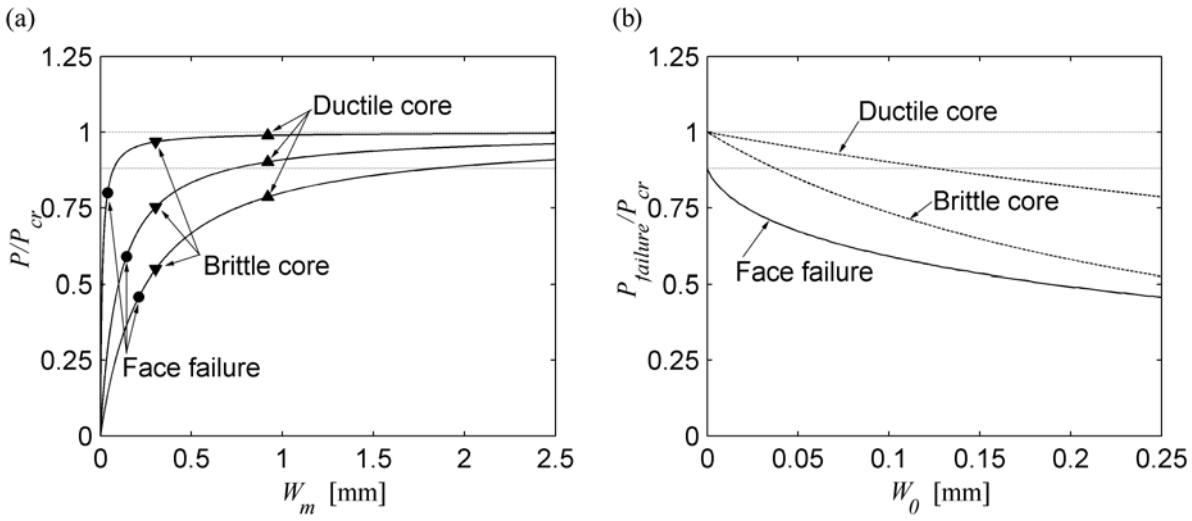

Figure 8. Example for a sandwich beam with1 mm UD Carbon and H200.
(a) Equilibrium paths for various imperfection amplitudes of 0.01, 0.1 and 0.25 mm.
(b) Face and core failure envelopes vs. initial imperfection amplitudes.

In this case face failure occurs prior to core failure for all imperfection amplitudes and for both ductile and brittle core materials. An additional horizontal line is drawn in both Figure 8a and 8b representing pure compression failure of the face sheet (Equation (19)). In Figure 8a it is obvious that the previously mentioned imaginary line through the face sheet failure markers crosses the load axis at the compression failure load of the face sheet for W_m equal to zero.

Comparison with FE-calculations

Finite element (FE) calculations where performed using the commercial FE code ABAQUS Standard [14] and the results where compared with the developed theory. A 2D model with quadratic beam and membrane elements were used to model a "unit cell" of the sandwich under wrinkling. The boundary conditions of the cell were chosen so the cell is repeatable and can build a sandwich in basic wrinkling (thick core). Coupled boundary conditions were used to keep the vertical edges (A-D and B-C) straight and vertical and also the bottom boundary (D-C) straight and horizontal, see Figure 9a. The beam elements at the top of the model are free except the two corner nodes (A and B) whose rotation is locked. To lock the last rigid body motion of the model, the top central node (E) is locked in both vertical and horizontal direction. Figure 9a shows both the mesh of the model and also a contour plot of the vertical stress distribution in the core for a post-buckled state (deformation strongly amplified).

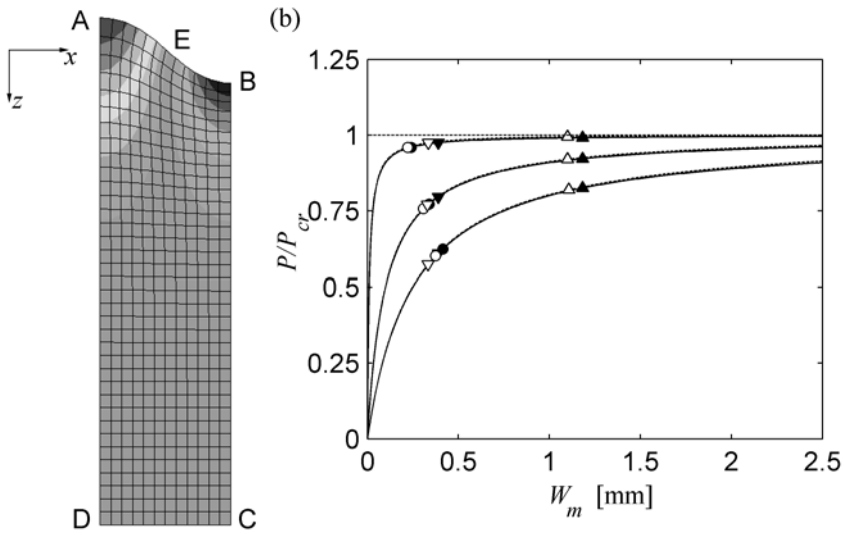

Figure 9. (a) Finite element model and (b) equilibrium paths with predicted failure markers; filled markers – model, open markers –FE predictions.

First a parametric study solving the linear eigenvalue problem was used to find the critical wavelength and correct model size for each particular material combination. Thereafter a nonlinear analysis using the obtained eigenmode as a perturbation of the model was performed. The different imperfection amplitudes were used to scale the amplitude of the eigenmode and the equilibrium paths obtained are very close to the ones previously predicted. In Figure 9b an example of the finite element calculations are compared to the analytical theory. The material properties used in the example are the same as in the second calculation example (1 mm unidirectional carbon fibre vinylester face sheet on a core with properties comparable to Divinycell H100, compare Figure 9b with 7a). Both the analytical equilibrium paths and those obtained by finite elements are drawn. The analytical ones are in solid lines and the ones from finite elements are dashed. They are so close to each other that it is difficult to separate them. The failure loads predicted using finite element calculation are also shown in the same figure as open markers. The face failure load predicted by finite element calculations are shown by open circles and core failure with open triangles. As the figure shows, the developed theory show very good agreement with the finite element calculations. The theory is slightly non-conservative for both face and core failure but this was anticipated since the change in wavelength is neglected in the theory. In reality the wavelength decreases as the effective wrinkling amplitude increases and this gives rise to an increase both in core and face strains in the compressed imperfect sandwich.

More comparisons between finite element analysis and the proposed model where performed and give very similar results to what is described above. They all support the presented theory although a somewhat larger (but still very small) discrepancy could be seen between the equilibrium paths for high stiffness core material. This increased discrepancy is probably again due to the neglected change in wrinkling wavelength between the loaded and unloaded sandwich. Even though there is not a perfect match of the results between finite element calculations and the developed theory, the correlation is very good and the finite element results strongly support the developed theory.

Moreover, the FE calculations give some additional interesting results. Even with a completely symmetric model the amplitudes of the face and core stresses differ between the

left and right part of the model. The face stress is higher in the rightmost corner, point B in Figure 9a and Figure 5. The absolute core stress is higher in the leftmost corner, point A in Figure 9a and Figure 5. This would to some degree explain why core rupture is common while core crushing is not. This behaviour can also be explained by the fact that the failure strain of most core materials differs in tension and compression.

Comparison with tests

The developed theory was compared to experimental results. The first test series consisted of small sandwich plates, 150 by 100 mm, with a carbon fibre vinylester face sheets on a range of 50 mm thick Divinycell H-grade core materials. The specimens were manufactured using a vacuum infusion technique giving high quality sandwich plates with a fibre fraction in the face sheets of about 0.6 (60%). The face sheet was built up of four layers with the outer laminae perpendicular to the inner, with a total thickness of 1 mm. The specimens were thereafter cut from the manufactured panels in two directions giving specimens with both $[0/90]_s$ and $[90/0]_s$ lay-ups. Subsequently the specimens were fitted with tabs and carefully milled to ensure that all loaded edges where flat and parallel to each other. For compression testing this last step is very important and strongly affects the reliability of the test results. The specimens were thereafter tested in an Instron test machine (displacement controlled) and the failure load was recorded. All specimens, except one, failed close to the predicted load and all failed by face fracture. One core rupture was observed but this is believed to be a secondary failure after the opposing face sheet already had failed. These experimental findings support the developed theory, which also predicts face failure for both face sheet configurations ([0/90]s and [90/0]s) and all tested core densities. The results from this test series were also published in [15]. The material properties for the face sheet were obtained by tensile testing of strips of the face sheet material. The core properties used in the calculations where taken from the technical specifications from the manufacturer, Divinycell International AB [16].

The results of the experiments compared to a traditional approach of comparing with the standard wrinkling formula, Equation (9) and with the face compression failure stress along with the present method is shown in Figure 10. The failure load is given as load per unit width of the face sheet. From the experimental results, the load carried by the core has been subtracted since this (though rather small contribution) is not included in the theory. The classical wrinkling load is given by dashed lines and so also the horizontal line corresponding to face compression failure load. From this classical approach, one can see that as the core modulus increases there is a failure mode shift from wrinkling to face sheet compression failure, as discussed in [15]. The present theory is presented by two shaded areas; one for each face sheet configuration. The upper boundary corresponds to an initial imperfection of 0.01 mm and the lower boundary to an initial imperfection of 0.25 mm. In reality, the imperfection amplitude should lie within these boundaries.

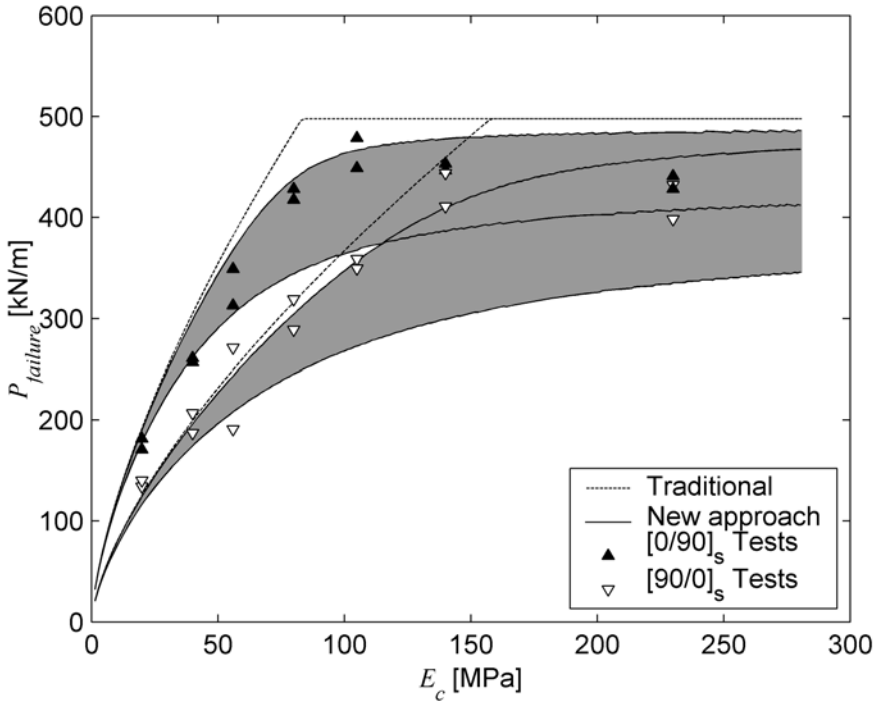

Figure 10. Developed theory compared to test results. [0/90]s and [90/0]s carbon fibre vinylester face sheet on Divinycell H-grade core material. Black triangles pointing up shows test results for $[0/90]_s$ specimens and white triangles pointing down show test results for $[90/0]_s$ specimens. Dashed lines are traditional theory (wrinkling and compression failure) and solid lines is the developed theory. The upper solid line for each material configuration corresponds to an initial imperfection amplitude of 0.01 mm and the lower line in each pair to 0.25 mm.

As can be seen from Figure 10, almost all test results lie within the assumed initial imperfection amplitude regime. This regime may appear relatively wide but it seems that the upper boundary (W_0 = 0.01 mm) is closer to the test results. One can further notice that the traditional approach of estimating the wrinkling load or the face sheet compression failure load is, in almost all cases, non-conservative. A photograph of a typical failed specimen from this test series is shown in Figure 11a.

A test series by Shipsha [17] included narrow (50 mm) beam specimens with a 2.4 mm thick glass-fibre vinylester face sheet (18 GPa Young's modulus, 0.3 Poisson ratio and 3% critical strain) on a 50 mm thick Rohacell WF51 core (85 MPa Young's modulus, 0.42 Poisson ratio and 3.3% critical strain). These specimens were tested under controlled displacement in an Instron machine and failed by core rupture at an average value of 620 kN/m per unit width and face sheet, equivalent to 92% of the critical load predicted by Allen's wrinkling formula, Equation (9). The present theory predicts failure by core rupture between 85% (0.1 mm imperfection amplitude) and 98% (0.01 mm imperfection amplitude) of the classical wrinkling load following Equation (9). A photograph of one failed test specimen from this series in shown in Figure 11b.

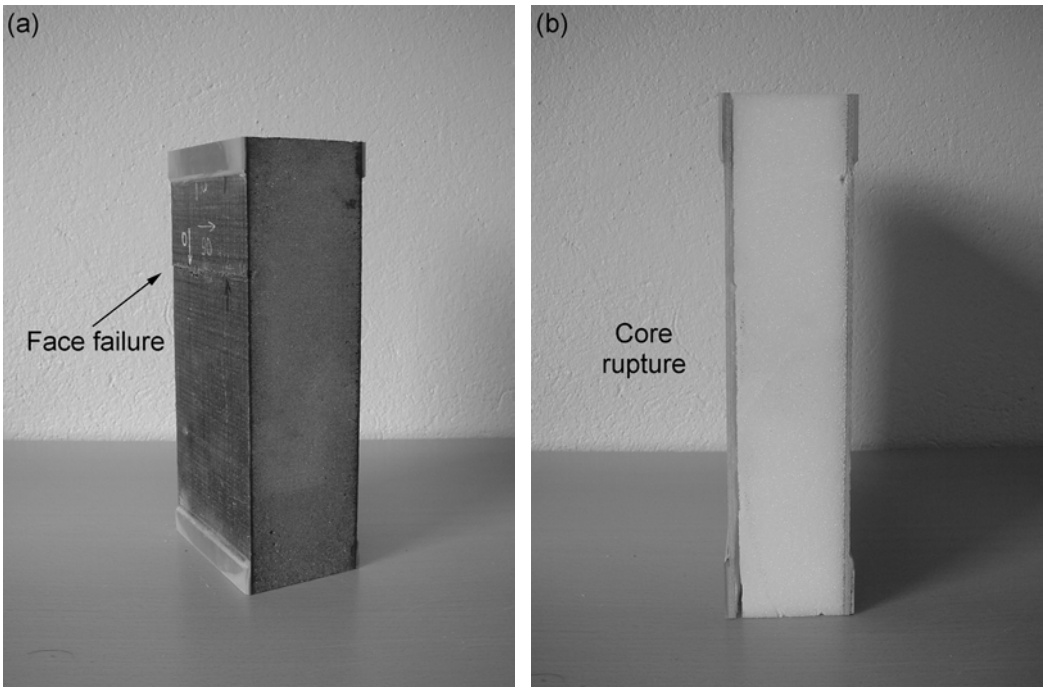

Figure 11. Photo of two of the tested specimens. (a) $[0/90]_s$ carbon fibre and vinylester face sheet on H60 core that failed by face failure. (b) 2.4 mm GFRP on WF51 core material that failed by core rupture.

Also these tests comply very well with the proposed theory and if a reasonably large imperfection amplitude is used in the calculations a conservative estimation of the failure load is obtained which include the transition from pure wrinkling to pure compression failure.

Design issues on efficiency

We shall now discuss the usage of the model and obtained results in the context of design. One can see from Figure 10 that the largest relative discrepancy between the traditional approach versus the new model and experimental results are in the regime where the traditional approach predicts a failure mode shift from wrinkling to face sheet compression failure. For low stiffness cores, say $E_c \leq 50$ MPa, the new model and test results compare very well with the traditional wrinkling load estimating, Equation (9). For high stiffness core, say $E_c \geq 150$ MPa, the failure load is quite close to the predicted face sheet compression load. In these two regimes, there seems to be no great need for additional knock-down of the traditional formulae. However, in the intermediate regime, the required knock-down is considerably larger. It must be mentioned, however, that the map of results in Figure 10 is for one single case and this may become quite different for another material combination.

Suppose that the "efficiency" is defined as the quotient between the actual load bearing capacity according to the model and the load bearing capacity according to the traditional approach, the latter being either the wrinkling load according to Equation (9) or the load for face sheet compression failure. The efficiency is then

$$Efficiency = \frac{P_{failure}}{P_{traditional}} \tag{28}$$

We can now calculate this efficiency for the case of a unidirectional carbon fibre face sheet using the same data used for the example in Figures 6-8. The results are given in Figure 12a for an initial imperfection amplitude of 0.1 mm, i.e. 1/10 of the face sheet thickness.

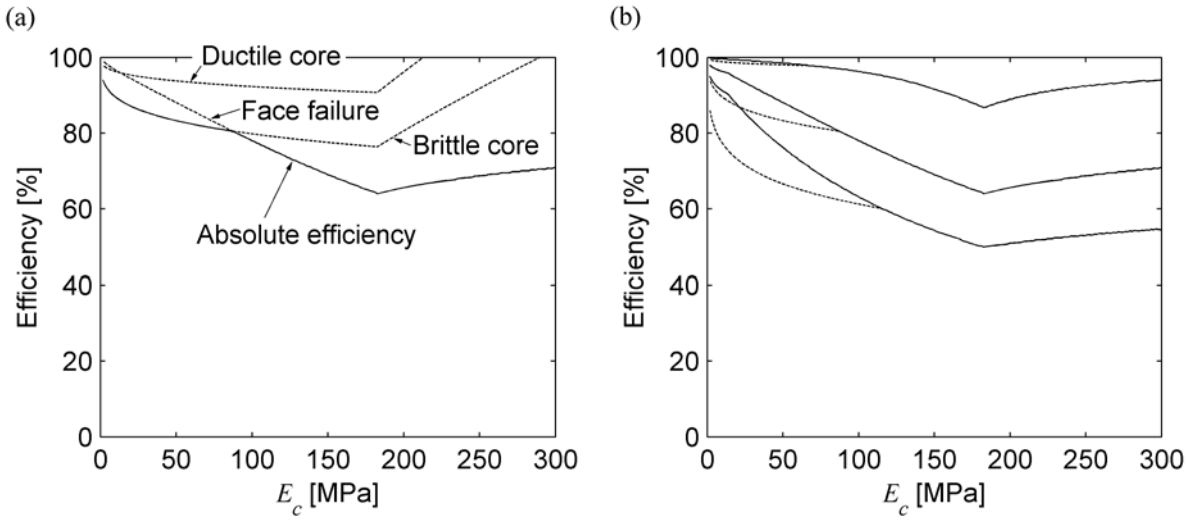

Figure 12. (a) Example of efficiency for a unidirectional carbon fibre face sheet sandwich with either a ductile core or brittle core with an initial imperfection amplitude of 0.1mm. (b) Efficiency factors for unidirectional carbon sandwich with ductile or brittle core with initial imperfection amplitudes of 0.01, 0.1 and 0.25 mm.

In the case of a ductile core, the transition from core rupture to face failure occurs for a fairly low modulus core ($E_c \leq 10$ MPa). The failure load according to the new model then drops compared to the wrinkling load of Equation (9) rather rapidly for a core material modulus up to about 180 MPa. In this regime ($E_c \leq 180$ MPa), the traditional approach predicts wrinkling to occur prior to face sheet compression failure. This almost straight line up to $E_c \leq 180$ MPa actually corresponds to the required knock-down factor for Equation (9). At about $E_c = 180$ MPa, the traditional approach predicts a shift in failure mode to face sheet compression failure, explaining the slope shift in the efficiency curve for face failure. From this point on, the efficiency increases again. For a brittle core, the first mode shift appears for a higher E_c, that is when the imperfection induced material failure shifts from core rupture to face sheet failure. In either case, the poorest efficiency occurs at around $E_c = 180$ MPa, where the actual failure load is only about 60% of that predicted by any traditional approach. Thus, from a design perspective, the point where the traditional approach suggest to be the most efficient design – where wrinkling and face sheet compression failure occurs at the same load, instead appears to be a rather poor design point, the point where the traditional approach requires the largest knock-down. It appears more efficient to design to a specific failure mode, away from this transition point, ensuring either wrinkling induced failure with a low knock-down factor or using a higher modulus core to ensure face sheet compression failure.

Figure 12b shows the same results as Figure 12a for the same face sheet and for both ductile and brittle core (dashed lines in Figure 12b), but for a number of different initial imperfection amplitudes; 0.01, 0.1 and 0.25 mm, respectively. The effect of the initial imperfection amplitude is of course that the required knock-down factor for the wrinkling formula of Equation (9) increases with increasing amplitude. However, the efficiency still has a minimum for the same core stiffness, in this case about $E_c = 180$ MPa.

Figure 13 shows the efficiency relations for the configuration used in the experiments, one being a $[0/90]_s$ laminate with a thickness of 1 mm with a ductile core type (Divinycell H-grade), and the other having glass fibre composite faces with a thickness of 2.4 mm and a brittle core type (Rohacell WF-grade). The assumed initial imperfection amplitude is 1/10 of the face sheet thickness, or 0.1 and 0.25 mm.

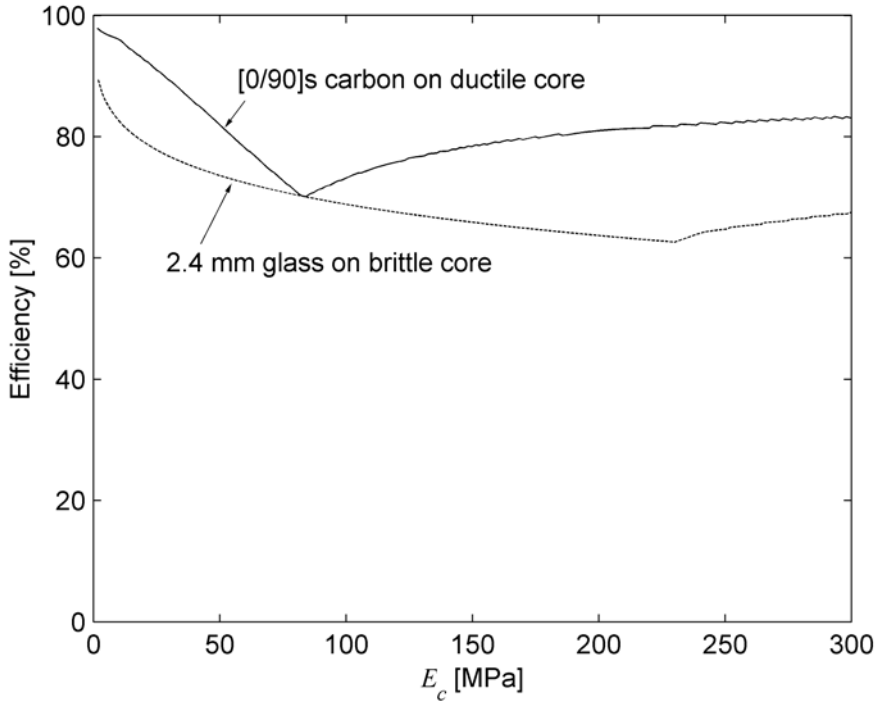

Figure 13. Efficiency factors for unidirectional carbon sandwich ductile core (Divinycell H-grade) with an initial imperfection amplitude of 0.1 mm, and quasi-isotropic glass sandwich with brittle core (Rohacell WF-grade) with an initial imperfection amplitude of 0.25 mm.

In Figure 13, the carbon/ductile core configuration is predicted to fail by wrinkling induced core rupture for very low core stiffness ($E_c \leq 10$ MPa) and above this the failure mode should be wrinkling induced face compression failure. The efficiency drops almost like a straight line down to approximately 70% of the traditional prediction. At this point the traditional approach predicts face sheet compression failure and then the efficiency starts to increase. In the glass/brittle core configuration, the predicted failure mode is core rupture in the entire core stiffness regime. The efficiency drops more dramatically for low stiffness cores, but the minimum value is still around 70% of the traditionally predicted wrinkling load. Note, however, that this configuration was given a larger initial imperfection amplitude.

Discussion and conclusions

The present paper investigates the effect of initial imperfections on the wrinkling load of composite foam core sandwich panels. This is done by deriving relations based upon classical wrinkling analyses approaches and combining these with first order extensions of finite deformations. This leads to simple relations for finding the load-deformation response. These are compared with FE calculations and tests and were found to correlate very well. The used

approach transforms the analysis from that of stability to a standard strength of materials analysis where face sheet compressive failure or core rupture are the assumed failure modes. Thus, wrinkling induced by initial imperfections become a strength problem rather than a stability problem. A number of examples were examined showing how failure transforms from face sheet compression to core rupture depending on the properties of the face sheet and the core material, including both stiffness and strength properties. Finite deformation finite element analysis was also used to compare with the model and gave excellent correlation. Finally, the presented model was compared to experimental results. It seems that a small assumed initial imperfection amplitude makes the model correlate well with the experimental results. The model gives much better predictions of wrinkling failure than the traditional approach using stability based wrinkling formulae. The presented model does, for the first time, give insight as to why traditional stability based wrinkling analysis is non-conservative and why knock-down factors must be used for these in reality. It appears that the knock-down factor to be used in traditional wrinkling analysis is a function of both the face sheet and core material properties, including both stiffness and strength properties. However, the derived model can be used to predict this knock-down, or even better, predict the actual failure load directly. The only remaining question is how to choose an appropriate initial imperfection amplitude. This depends clearly on material and manufacturing issues, such as what kind of fabrics are used and the choice of manufacturing method.

A traditional design analysis implies, as mentioned previously, that one would try to find a design where the wrinkling load equals that of the face sheet compression failure load and from that choose a core material modulus. However, the findings of this paper imply otherwise. In fact, it is seen that the utilisation of the material actually is the poorest at this very design point. At this point, we find that the difference in estimated wrinkling load has a maximum comparing the traditional method and the new one presented herein. This can be seen not only from the presented model, but also by analysing experimentally measured failure loads.

From the analysis and following the discussion above on material usage efficiency it appears that a good design is when the traditional wrinkling load is higher than the load required to cause face sheet compression failure. Doing this requires a higher modulus, and thus higher density core, which obviously adds weight. One can of course, using the presented model, perform similar efficiency calculations based on structural weight. However, it is important to remember that such an analysis or optimization procedure should include all other requirements for the sandwich panel; global stiffness, global buckling, load carrying capacity, natural vibrations, etc.

The analysis presented in this paper is based on assuming some initial imperfection amplitude, the shape being assumed to coincide with the natural wrinkling wave shape, thus assuming some sort of worst-case scenario. The imperfection amplitude greatly influences the load bearing capacity of the sandwich panel. A small amplitude, say 1/100 of the face sheet thickness will however reduce the strength of a panel compared to what may be anticipated assuming wrinkling instability as a failure mode. Larger amplitudes, say 1/10 of the face sheet thickness, will drastically reduce the load bearing capacity, in our presented cases down to as much as 60% of the traditional wrinkling load. The model presented herein is asymptotically correct in the sense that if the imperfection amplitude approaches zero, the failure load approaches the traditional failure load being the lower of wrinkling and compression failure.

To design a sandwich less sensitive to imperfections a few guidelines are good to bear in mind. The first is not to use too thin face sheets. A thin face sheet is more affected by a small imperfection then a thicker face sheet. The second is to use materials with high strain to failure to prevent abrupt failure at a too low a load. The third and least obvious guideline is to design away from the transition point between traditional wrinkling and compression failure.

Acknowledgements

This work was funded by The Swedish Defence Materiel Administration, FMV Contract 63823-LB109101, and was conducted with support from Kockums AB Karlskronavarvet.

References

[1] Hoff N.J. and Mautner S.E., "Buckling of Sandwich Type Panels", *Journal of the Aeronautical Sciences*, Vol. 12, No 3, pp. 285-297, 1945.

[2] Plantema F.J., *Sandwich Construction*, John Wiley & Sons, New York, 1966.

[3] Dawe D.J. and Yuan W.X., "Overall and local buckling of sandwich plates with laminated faceplates, Part I: Analysis", *Computer methods in applied mechanics and engineering*, Vol. 190, pp. 5197-5213, 2001.

[4] Allen H.G., *Analysis and Design of Structural Sandwich Panels*, Pergamon Press, Oxford, 1969.

[5] Niu K. and Talreja R., "Modeling of Wrinkling in Sandwich Panels Under Compression", *Journal of Engineering Mechanics*, Vol. 125, pp. 875-883, 1999.

[6] Vonach W.K., Rammerstorfer F.G., "Wrinkling of thick orthotropic sandwich plates under general loading conditions", *Archive of Applied Mechanics*, Vol. 70, pp. 338-348, 2000.

[7] Hadi B.K., "Development of Benson-Mayers theory on the wrinkling of anisotropic sandwich panels", *Composite Structures*, Vol. 49, pp. 425-434, 2000.

[8] Fagerberg L. and Zenkert D., "Effects of anisotropy and multi-axial loading on the wrinkling of sandwich panels", submitted, 2003.

[9] Zenkert D., *An Introduction To Sandwich Construction*, EMAS Ltd, Warley, UK, 1995.

[10] Fagerberg L., "The effect of local bending stiffness on wrinkling of sandwich panels", *Journal of Engineering for the Maritime Environment*, Vol. 217, pp. 111-119, 2003.

[11] Grenestedt J.L. and Olsson K.-A., "Wrinkling of Sandwich Panels with Layered Core or Non-symmetric Skins", *Proc. 5:th International Conference on Sandwich Construction*, Ed. H.G. Allen, EMAS Ltd., Warley, UK, 1995.

[12] Timoshenko S.P. and Gere J.M., *Theory of Elastic Stability*, Second Edition, McGraw-Hill, New York, 1961.

[13] Brush D.O. and Almroth B.O., *Buckling of Bars Plates and Shells*, McGraw-Hill, New York, 1975.

[14] Hibbitt, Karlsson & Sorensen, Inc., *ABAQUS/Standard User's Manual*, 1080 Main Street, Pawtucket, RI 02860-4847, U.S.A., http://www.abaqus.com.

[15] Fagerberg L., "Wrinkling and compression failure transition in sandwich panels", Report 2002-35, *Accepted for publication in Journal of Sandwich Structures and Materials*, August 2002.

[16] Divinycell International AB, *H grade Technical Specifications*, Box 201, SE-312 22 Laholm, Sweden, http://www.divinycell.se.

[17] Shipsha A., Hallström S. and Zenkert D., "Failure Mechanics and Modelling of Impact Damage in Sandwich Beams – A 2D Approach: Part I – Experimental Investigation", *Journal of Sandwich Structures and Materials*, Vol. 5, pp.7-31, January 2003.